Photoemission evidence for a Mott-Hubbard metal-insulator transition in VO_2

R. Eguchi,[1,*] M. Taguchi,[1] M. Matsunami,[1] K. Horiba,[1] K. Yamamoto,[1] Y. Ishida,[1] A. Chainani,[1] Y. Takata,[1] M. Yabashi,[2,3] D. Miwa,[2,†] Y. Nishino,[2] K. Tamasaku,[2] T. Ishikawa,[2,3] Y. Senba,[3] H. Ohashi,[3] Y. Muraoka,[4] Z. Hiroi,[4] and S. Shin[1,4]

[1]*Soft X-Ray Spectroscopy Laboratory, RIKEN SPring-8 Center, Sayo-cho, Sayo-gun, Hyogo 679-5148, Japan*

[2]*Coherent X-Ray Optics Laboratory, RIKEN SPring-8 Center, Sayo-cho, Sayo-gun, Hyogo 679-5148, Japan*

[3]*JASRI/SPring-8, Sayo-cho, Sayo-gun, Hyogo 679-5198, Japan*

[4]*Institute for Solid State Physics, University of Tokyo, Kashiwanoha, Kashiwa, Chiba 277-8581, Japan*

(Received 3 June 2008; revised manuscript received 23 July 2008; published 18 August 2008)

The temperature (T)-dependent metal-insulator transition (MIT) in VO_2 is investigated using bulk sensitive hard-x-ray ($\sim$8 keV) valence-band, core-level, and V $2p-3d$ resonant photoemission spectroscopies (PESs). The valence-band and core-level spectra are compared with full-multiplet cluster model calculations including a coherent screening channel. Across the MIT, V $3d$ spectral weight transfer from the coherent ($3d^1\underline{C}$ final) states at Fermi level to the incoherent ($3d^0+3d^1\underline{L}$ final) states, corresponding to the lower Hubbard band, leads to gap formation. The spectral shape changes in V $1s$ and V $2p$ core levels as well as the valence band are nicely reproduced from cluster model calculations, providing electronic structure parameters. Resonant PES finds that the $3d^1\underline{L}$ states resonate across the V $2p-3d$ threshold in addition to the $3d^0$ and $3d^1\underline{C}$ states. The results support a Mott-Hubbard transition picture for the first-order MIT in VO_2.

DOI: 10.1103/PhysRevB.78.075115 PACS number(s): 79.60.−i, 71.30.+h

VO_2, a $3d^1$ electron system, exhibits a sharp first-order metal-insulator transition (MIT) as a function of temperature (T) at T_{MI}=340 K.[1] The high-T metal phase has a rutile (R) structure, while the low-T insulating phase has a monoclinic (M_1) structure with zigzag-type pairing of V atoms along the c axis.[2] Magnetically, the metallic R phase shows enhanced susceptibility (χ) with an effective mass $m^*/m\sim 6$, while the insulating M_1 phase is nonmagnetic. Consequently, VO_2 has attracted enormous attention in terms of a Mott-Hubbard (MH) correlation-induced versus a structural Peierls-type MIT.

Goodenough[3] proposed that the lowest-energy t_{2g} states split into the $d_\parallel$ band and the π^* bands. In the R phase, the $d_\parallel$ band overlaps the π^* band. In the M_1 phase, the zigzag-type pairing consists of (i) a tilting of the V-V pairs which lifts the π^* band above the Fermi level (E_F), and (ii) the $d_\parallel$ band opens up a gap because of the splitting into a filled bonding and empty antibonding band caused by V-V pairing. Zylberstejn and Mott[4] attributed the MIT to an on-site Hubbard-type Coulomb energy U in the $d_\parallel$ band. Pouget and co-workers[2,5] showed that pure VO_2 under uniaxial stress and Cr-doped VO_2 exhibit an insulating (M_2) phase, in which half of the V atoms form pairs and the other half form zigzag chains that behave as spin-1/2 Heisenberg chains in NMR and EPR experiments.[6] Another intermediate phase [triclinic (T_r)] connecting $M_2\rightarrow M_1$ showed a bonding or dimerization transition of the Heisenberg chain V atoms with a concomitant decrease in χ. Thus, it was concluded that the M_1 insulating phase of VO_2, as well as the M_2 and T_r phases, is MH insulators. In an alternative picture, VO_2 was explained in terms of a Peierls insulating phase due to the structural phase transition. The electron-phonon interaction was considered to be important from Raman scattering[7] and x-ray-diffraction studies.[8] An *ab initio* molecular-dynamics study in the local-density approximation (LDA) described VO_2 as a charge-ordered band (Peierls) insulator,[9] but a genuine gap was not obtained. Also, the linear resistivity of metallic VO_2, analyzed in terms of an electron-phonon effect in a Fermi liquid, gives an invalid mean free path (MFP).[9] The LDA approach for VO_2 was discussed in comparison with NbO_2 and MoO_2 but does not provide a gap in the density of states (DOS).[10] Combining O $1s$ x-ray absorption spectroscopy (XAS) and ultraviolet (UV)–photoemission spectroscopy (PES), the value of the $d_\parallel$ band splitting was estimated to be 2.6 eV, whereas the LDA calculates it to be 2.0 eV. The authors concluded that the structural distortion is dominantly responsible for the $d_\parallel$ band splitting in the insulating phase.[11]

The gap in the DOS and suppressed moment are correctly obtained in the cluster dynamical mean-field theory (c-DMFT) calculations of Biermann *et al.*,[12] showing the crucial role of strong Coulomb interactions and structural distortions in VO_2. The c-DMFT gives an isotropic metal, with the d electron occupancy: 0.42 in the $d_\parallel$ ($\equiv a_{1g}$) band and 0.29 each in the π^* ($\equiv e_g$ doublet) bands. In the insulating phase, occupancies change to 0.8 in the $d_\parallel$ ($\equiv a_{1g}$) band and $\sim$0.1 in each of the π^* ($\equiv e_g$ doublet) bands. Biermann *et al.*[12] concluded that VO_2 exhibits *a correlation-assisted Peierls transition*. Haverkort *et al.*,[13] using polarization dependent XAS, showed the importance of orbital occupancy switching in the V $3d$ states across the MIT, in very good agreement with the occupancies calculated in a cluster model, as well as c-DMFT results. Haverkort *et al.*[13] concluded an *orbital-assisted collaborative Mott-Peierls transition* for VO_2.

VO_2 has provided other important results: an electric-field-induced MIT (Ref. 14) and a photoinduced MIT.[15] The electric-field-induced MIT, in the absence of a structural transition, favors a MH transition. From the ultrafast ($<$ps) time scale of the photoinduced MIT in VO_2,[15] the study concluded that the accompanying structural transition may not be thermally initiated. In VO_2/TiO_2:Nb thin films, the photoinduced electron-hole pairs result in a reduced resistivity by 10^{-3} times in the insulating phase and a surface photovoltage effect.[16] We recently reported the photoinduced electronic structure changes using soft-x-ray (SX)-PES, showing the combined effects of rigid-band behavior and correlation effects.[17] Several PES studies[17–22] have addressed

the electronic structure changes across the T-dependent MIT in VO_2. Early work discussed the role of strong correlations versus structural effects in VO_2.[18–20] A T-dependent UV-PES study with an analysis of surface and bulk components suggested the importance of both electron-electron and electron-phonon interactions for the electronic structure of VO_2.[21] More recently, infrared spectroscopy and nanoscale microscopy was used to reveal a divergent quasiparticle mass of the metallic carriers an approaching the insulating phase.[23] The insulating phase of VO_2 was classified as a Mott insulator with charge ordering. Thus, we felt it important to study the MIT in VO_2 using bulk sensitive hard-x-ray (HX)-PES, complemented by full-multiplet cluster calculations and V $2p-3d$ resonant PES. Recent studies using HX-PES have shown new features in core-level spectra which could be consistently explained in terms of well-screened peaks.[24–26] A study on valence band and core levels of V_2O_3 using HX-PES has shown a clear correlation between the well-screened peak and the coherent peak at E_F.[27] Theoretical studies have also shown the importance of coherent screening[28] as well as nonlocal screening[29] in core-level spectra.

In this work, we study VO_2 thin films using HX-PES ($h\nu$=7937 eV). Since the MFP of electrons using HX-PES is significantly longer (6–10 nm) than that using UV or SX-PES (<2 nm),[30] it provides the bulk electronic structure. However, the photoionization cross sections (PICSs) become very small ($\sim 10^{-5}$ times) compared to UV or SX photons and severely limit valence-band studies. In order to enhance signal intensity and since HX attenuation lengths are much longer than relevant MFPs, we adopted a grazing incidence geometry.[31] This necessitated the use of VO_2 thin films grown on a single-crystal surface of TiO_2:Nb, allowing us an incidence angle of about 1°. We measure the valence band, the V $1s$, V $2p$, and O $1s$ core-level spectra as a function of T. Resonant PES across the V $2p-3d$ threshold, and a cluster model calculation of the valence-band and the core-level V $1s$ and V $2p$ spectra provide a consistent picture of electronic parameters for VO_2.

A 10-nm-thick VO_2 film was epitaxially grown on the (001) surface of 0.05 wt % Nb-doped TiO_2 single-crystal substrates using the pulsed laser deposition technique, as described elsewhere.[32] The tensile strain results in a first-order hysteretic transition just like bulk VO_2 but at a slightly lower temperature of $T_{MI} \sim 292$ K. HX-PES and SX-PES experiments were carried out at undulator beam line BL29XUL SPring-8 (Ref. 33) using a Gammadata-Scienta R4000-10 kV spectrometer[31] and BL17SU SPring-8 using a Gammadata-Scienta SES2002 spectrometer.[34] The energy resolution was set to 200–250 meV. The measurements were carried out in a vacuum of 5×10^{-8} Pa at 270 and 320 K. E_F of VO_2 was referenced to that of a gold film evaporated onto the sample holder in all measurements.

Figure 1(a) shows the raw data of the entire valence band of VO_2 measured using HX-PES at 320 and 270 K, normalized for area under the curve. The valence-band structure consists of the dominantly V $3d$ band near E_F (0–2.5 eV binding energy) and a broad band usually considered as the dominantly O $2p$ band between 3 and 10 eV in previous results.[19,21] Based on PICS and a comparison with SX-PES results,[22] the spectral shape of the 7.5 eV feature suggests

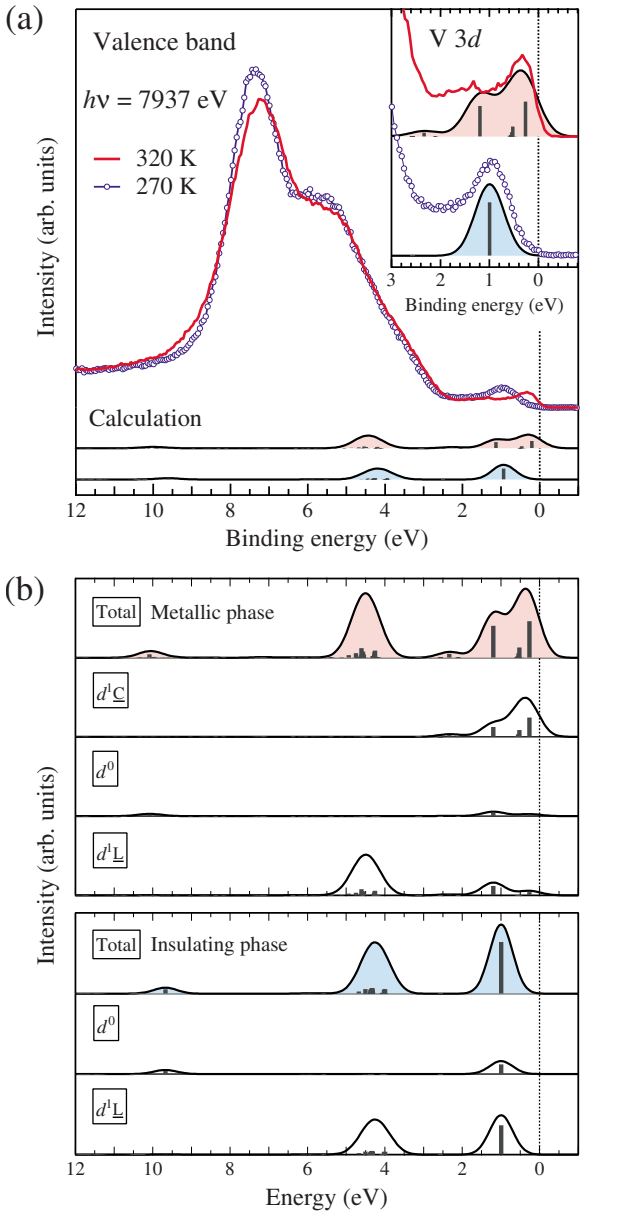

FIG. 1. (Color online) (a) Valence-band spectra measured across the MIT using hard x ray ($h\nu$=7937 eV) compared with the cluster model calculation. Inset shows an expanded view (0–3 eV) of the V $3d$ states near E_F. (b) The main final-state configuration spectra in the metallic phase and the insulating phase.

that the V $4s$ contribution overlaps the O $2p$ states. The energy position and width of the so-called O $2p$ band change slightly across the MIT, consistent with SX-PES results.[22] Figure 1(a) (inset) shows an expanded view (0–3 eV) of the V $3d$ states near E_F, which provides a direct picture of the gap formation in VO_2. The 320 K spectrum shows a peak centered at 0.3 eV and a clear Fermi edge, indicating the metallic state, and another broad weak feature centered at about 1.5 eV. These features correspond to the coherent band at E_F and the incoherent (lower Hubbard) band, respectively. The larger intensity in the near E_F DOS using HX-PES is attributed to the bulk sensitive V $3d$ states since the PICS of V $3d$ is higher than O $2p$ at high-photon (high-kinetic) en-

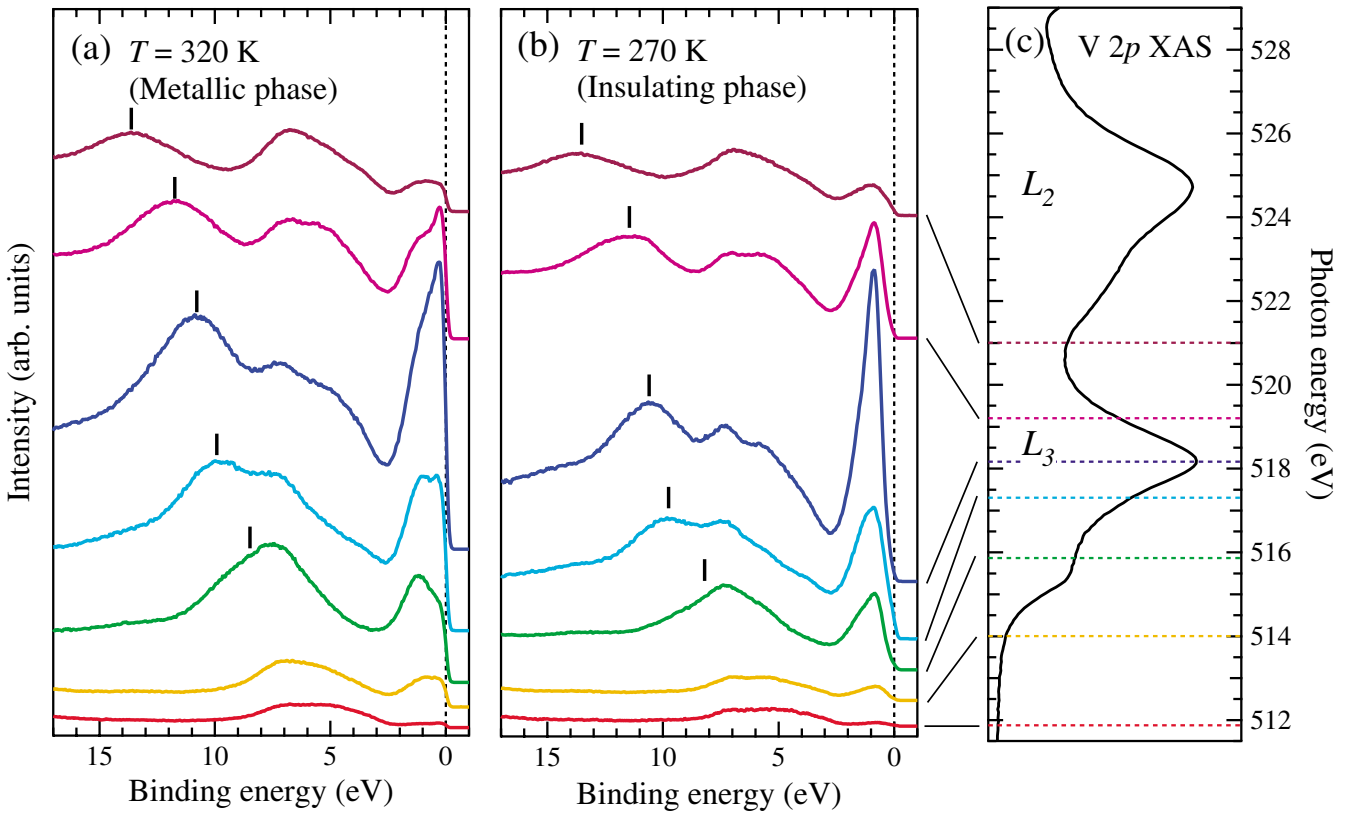

FIG. 2. (Color online) Resonant PES across the V $2p-3d$ threshold in (a) the metallic phase and (b) the insulating phase. (c) V $2p$ XAS spectra.

ergy. The 270 K spectrum near E_F shows large changes compared to the 320 K spectrum with a peak centered at 1 eV and negligible intensity at E_F, indicative of an energy gap of about 0.2 eV.

Moreover, in order to investigate the origin of these structures in detail, we carried out calculations for a VO_6 cluster model in O_h symmetry, as described in earlier work.[24,35] For simplicity, we assume a octahedral symmetry throughout. Since the crystal-field effect on peak intensities and positions in photoemission is small even for the (generally dominant) cubic contribution, it is clear that the neglected lower-symmetry terms would not change the spectral shapes in any significant way as far as photoemission is concerned. A study of lower symmetry is beyond the scope of this work. In addition to the usual charge-transfer (CT) energy Δ from the O $2p$ ligand band to the upper Hubbard band, the charge-transfer energy from the coherent band to the upper Hubbard band is defined as Δ^*. The ground state is described by a linear combination of following configurations: $3d^1$, $3d^2\underline{L}$, $3d^3\underline{L}^2$, $3d^2\underline{C}$, $3d^3\underline{L}\underline{C}$, and $3d^3\underline{C}^2$. The parameters were set as follows: $\Delta=4.0$ eV, $\Delta^*=0.2$ eV, $U_{dd}=4.5$ eV, $10Dq=1.2$ eV, $V=2.4$ eV, and $R_v=0.8$ eV; in addition, $U_{dc}(1s)=8.0$ eV, $U_{dc}(2p)=6.5$ eV, $R_c(1s)=0.9$ eV, and $R_c(2p)=0.8$ eV for the core-level calculations [Figs. 3(b) and 3(c)]. Theoretical calculations for transition-metal impurities in a solid give a $U_{dd}\sim 7.5$ eV for V, which gets reduced by typically $\sim 60\%$ in an oxide.[36] The calculations reproduce the experimental spectra in the metallic and the insulating phases. All the parameters for the calculated spectra for the metallic and insulating phases are equal, except for the hybridization between the central V atom $3d$ orbitals and the coherent band, V^*. $V^*=0.48$ eV for the metallic phase, and it was set to $V^*=0$ eV for the insulating phase. This confirms the importance of the coherent screening channel in reproducing the metallic phase of VO_2. The discrete levels obtained from the calculations were broadened by a Gaussian function of full width at half maximum $\Delta E=0.35$ eV.

Figure 1(b) shows the main final-state configuration ($3d^1\underline{C}$, $3d^0$, and $3d^1\underline{L}$) spectra in the metallic and the insulating phase. The total spectra are also shown in Fig. 1(a). In the metallic phase, the coherent screening state $3d^1\underline{C}$ is dominant near the E_F. On the other hand, the locally screening $3d^0$ state has a large intensity at a binding energy of ~ 1 eV with weak contribution from $3d^1\underline{L}$ states. In insulating phase, the coherent screening states vanish and the locally screened $3d^0$ with $3d^1\underline{L}$ admixture states remains around 1 eV. This feature corresponds to the effective lower Hubbard band, nicely matching the incoherent band in PES spectrum. The main contribution of $3d^1\underline{L}$ state appears around 4 eV in the metallic and insulating phases. We have checked that the ground-state configuration is a mixed character (MH+CT) state. The difference compared to an earlier study[37] stems from a dominantly MH description in the present study compared to dominantly CT description in Ref. 37. Specifically, Mossanek and Abbate[37] used $\Delta=2.0$ eV and $U=4.5$ eV, while in the present case, we have used $\Delta=4.0$ eV and $U=4.5$ eV.

The single-site DMFT (Ref. 38) and the c-DMFT (Ref.

12) calculations both indicate large changes in charge redistribution across the MIT. The c-DMFT calculation predicts a weak intensity lower Hubbard band in the insulating phase at ~1.8 eV with the quasiparticle origin feature shifted to 0.8 eV for a $U=4$ eV and $J=0.68$ eV. However, the HX-PES shows no feature at ~1.8 eV, but a single peak at 1.0 eV that is attributed to $3d^0$ state (the lower Hubbard band) in the cluster model calculation result. The c-DMFT study points out that a lower U (e.g., 2 eV) also stabilizes a gap, provided J is also small. However, it probably implies that the quasiparticle feature will move to even smaller energies than 0.8 eV. Instead, a c-DMFT with a larger U and J is probably more appropriate for VO_2. As has been discussed, while single-site DMFT results can also give a gap with a large U (~5 eV), it also gives local moment. While additional calculations can provide quantitatively accurate comparisons, both the single site and c-DMFT would require a $U>4$ eV. Thus we have set $U_{dd}=4.5$ eV as a reasonable value in the present calculations.

Using XAS and resonant PES across the V $2p-3d$ threshold, we show the enhanced V $3d$ electronic structure. It resonates due to interference between the direct channel ($p^6d^n+h\nu \rightarrow p^6d^{n-1}+e$) and the photoabsorption channel ($p^6d^n+h\nu \rightarrow p^5d^{n+1} \rightarrow p^6d^{n-1}+e$) excitations. Resonant PES is well known for probing this behavior in correlated oxides such as NiO, CuO, etc., and f-electron systems.[39,40] Using photon energies marked in the XAS profile of Fig. 2(c), we measured valence-band PES in the metallic [Fig. 2(a)] and the insulating phase [Fig. 2(b)]. These spectra are normalized to the scan time and the incident photon flux. The off-resonance spectrum is very similar to the SX-PES spectrum.[17,18,22] The spectra show a typical resonance enhancement of the 0–2 eV feature as a function of $h\nu$ with a maximum at $h\nu=518.2$ eV (L_3 peak in XAS). This confirms $3d$ electron character of the 0–2 eV feature. Moreover, the higher-binding feature of O $2p$ band gets enhanced at a lower energy (~514 eV) and is further enhanced at 516 eV. At higher $h\nu$, a strong intensity Auger feature shows up at higher-binding energy and tracks the increase in $h\nu$ [marked in Figs. 2(a) and 2(b)]. The valence-band calculations suggest the existence of the main $3d^1\underline{L}$ state overlapping the O $2p$ band. It resonates due to interference between the direct channel ($d^2\underline{L}+h\nu \rightarrow d^1\underline{L}+e$) and the photoabsorption channel ($p^6d^2\underline{L}+h\nu \rightarrow p^5d^3\underline{L} \rightarrow p^6d^1\underline{L}+e$). Note that the $3d^1\underline{L}$ final-state position is not clearly fixed in the present calculation because the present cluster calculations give a discrete level for the $3d^1\underline{L}$, unlike actual $3d^1\underline{L}$ states having a band-like energy distribution. The Auger features are hardly observed in the 0–2 eV resonant feature, very similar to the case of Ti_2O_3 resonant PES, another $3d^1$ system.[41]

Figure 3(a) shows the O $1s$ core-level HX-PES spectra at 320 and 270 K. The O $1s$ core level shows clear spectral shape change; a symmetric peak in the insulating phase transforms to an asymmetric Doniach-Šunjić line shape in the metal phase. No contamination feature at higher binding energy to the main peak is observed. Figure 3(b) shows the V $2p$ core-level spectra at 320 and 270 K. The V $2p_{3/2}$ and V $2p_{1/2}$ main peaks are positioned at ~516 and ~524 eV. The V $2p$ spectra show remarkable changes across the MIT: the peak shape is sharp in the insulating phase but shows a shoulder structure at low binding energy in the metal phase. In addition, the V $1s$ core-level spectra at 320 and 270 K show very similar changes like the V $2p$ spectra, as shown in Fig. 3(c). The V $1s$ main peak is positioned at 5468 eV with a weak satellite at 5481 eV in the insulating phase. The main peak and the satellite feature get broadened in the metallic phase with clear additional structure at lower binding energies.

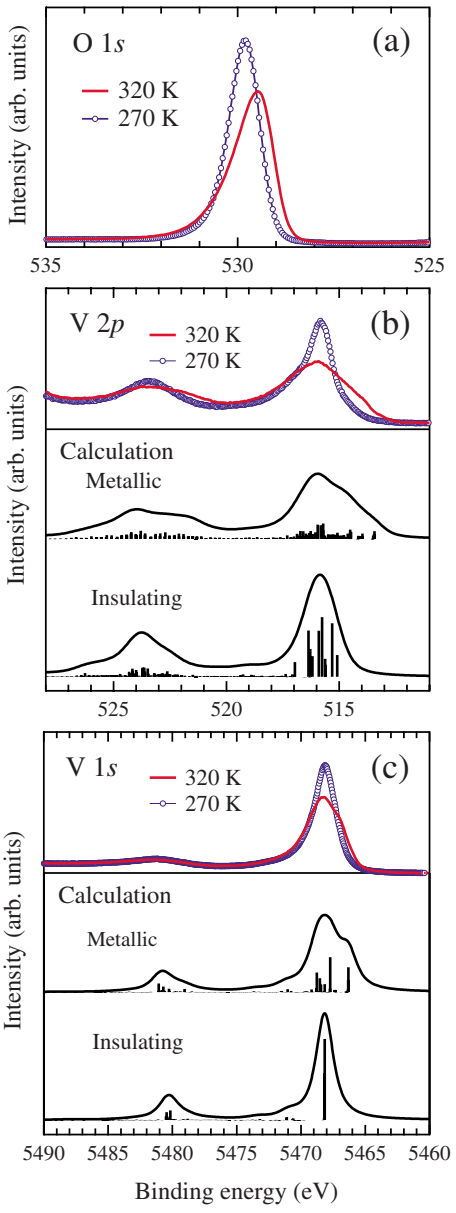

FIG. 3. (Color online) (a) O $1s$, (b) V $2p$, and (c) V $1s$ core-level spectra measured across the MIT using hard x ray ($h\nu=7937$ eV) compared with the cluster calculations for the metallic phase and the insulating phase.

We also carried out cluster calculations using the same set of parameters as for the valence-band calculations. The calculations [Figs. 3(b) and 3(c)] nicely reproduce the V $2p$ and V $1s$ core-level experimental spectra. The shoulder structure appears in the metallic spectrum, whereas the insulating phase spectrum has no shoulder structure in the V $1s$ as well as V $2p_{1/2}$ and V $2p_{3/2}$ core levels. The results confirm that

the screening channel from the coherent band at E_F is responsible for the shoulder structure. This result is slightly different from HX-PES results reported in V_2O_3 (Refs. 24 and 25) and $La_{1-x}Sr_xMnO_3$,[26] which show a clear additional peak derived from the coherent screening in both HX-PES core-level spectra and the cluster model calculations. Since the additional peak position is affected by the magnitude of the parameters, Δ, Δ^*, and U_{dc}, in the calculation,[24] the additional peak appear well separated from the main peak and the ligand screening ($2p^5 3d^n \underline{L}$) peak in V_2O_3 and $La_{1-x}Sr_xMnO_3$, resulting in a distinguishable peak structure. In contrast, since the Δ is relatively small compared to U_{dc} for VO_2, and unlike V_2O_3 and $La_{1-x}Sr_xMnO_3$, the coherent screening state is positioned near the ligand screening state, resulting in a broad shoulder structure. The overall calculation results thus reproduce the core-level and valence-band PES spectra and provide consistent electronic structure parameters with a $U \gtrsim \Delta$.

In conclusion, we have performed T-dependent valence-band and core-level HX-PES of VO_2. The valence-band spectra show gap formation and weight transfer from the coherent state (the quasiparticle band, $3d^2\underline{C} \rightarrow 3d^1\underline{C}$ character) to a mixed incoherent state [the lower Hubbard band, $(3d^1 \rightarrow 3d^0) + (3d^2\underline{L} \rightarrow 3d^1\underline{L})$ character], supporting a MH transition picture. Resonant PES across the V $2p-3d$ threshold finds that the $3d^1\underline{L}$ state, which overlaps the O $2p$ band, resonates as well as $3d^0$ and $3d^1\underline{C}$. The spectral shape changes in V $1s$ and V $2p$ core levels as well as the valence band are nicely reproduced from a cluster model, providing a consistent set of electronic structure parameters.

*ritsuko@spring8.or.jp
†Deceased.

[1] F. J. Morin, Phys. Rev. Lett. **3**, 34 (1959).
[2] J. P. Pouget, H. Launois, T. M. Rice, P. Dernier, A. Gossard, G. Villeneuve, and P. Hagenmuller, Phys. Rev. B **10**, 1801 (1974).
[3] J. B. Goodenough, J. Solid State Chem. **3**, 490 (1971).
[4] A. Zylbersztejn and N. F. Mott, Phys. Rev. B **11**, 4383 (1975).
[5] T. M. Rice, H. Launois, and J. P. Pouget, Phys. Rev. Lett. **73**, 3042 (1994).
[6] J. P. Pouget, H. Launois, J. P. D'Haenens, P. Merenda, and T. M. Rice, Phys. Rev. Lett. **35**, 873 (1975).
[7] R. Srivastava and L. L. Chase, Phys. Rev. Lett. **27**, 727 (1971).
[8] D. B. McWhan, M. Marezio, J. P. Remeika, and P. D. Dernier, Phys. Rev. B **10**, 490 (1974).
[9] R. M. Wentzcovitch, W. W. Schulz, and P. B. Allen, Phys. Rev. Lett. **72**, 3389 (1994); P. B. Allen, R. M. Wentzcovitch, W. W. Schulz, and P. C. Canfield, Phys. Rev. B **48**, 4359 (1993).
[10] V. Eyert, Ann. Phys. **11**, 650 (2002).
[11] R. J. O. Mossanek and M. Abbate, Solid State Commun. **135**, 189 (2005).
[12] S. Biermann, A. Poteryaev, A. I. Lichtenstein, and A. Georges, Phys. Rev. Lett. **94**, 026404 (2005).
[13] M. W. Haverkort, Z. Hu, A. Tanaka, W. Reichelt, S. V. Streltsov, M. A. Korotin, V. I. Anisimov, H. H. Hsieh, H.-J. Lin, C. T. Chen, D. I. Khomskii, and L. H. Tjeng, Phys. Rev. Lett. **95**, 196404 (2005).
[14] H.-T. Kim, B.-G. Chae, D.-H. Youn, G. Kim, K.-Y. Kang, S.-J. Lee, K. Kim, and Y.-S. Lim, Appl. Phys. Lett. **86**, 242101 (2005).
[15] A. Cavalleri, Cs. Tóth, C. W. Siders, J. A. Squier, F. Ráksi, P. Forget, and J. C. Kieffer, Phys. Rev. Lett. **87**, 237401 (2001); A. Cavalleri, Th. Dekorsy, H. H. W. Chong, J. C. Kieffer, and R. W. Schoenlein, Phys. Rev. B **70**, 161102(R) (2004); A. Cavalleri, M. Rini, H. H. W. Chong, S. Fourmaux, T. E. Glover, P. A. Heimann, J. C. Kieffer, and R. W. Schoenlein, Phys. Rev. Lett. **95**, 067405 (2005).
[16] Y. Muraoka, T. Yamauchi, Y. Ueda, and Z. Hiroi, J. Phys.: Condens. Matter **14**, L757 (2002).
[17] R. Eguchi, S. Shin, A. Fukushima, T. Kiss, T. Shimojima, Y. Muraoka, and Z. Hiroi, Appl. Phys. Lett. **87**, 201912 (2005).
[18] G. A. Sawatzky and D. Post, Phys. Rev. B **20**, 1546 (1979).
[19] S. Shin, S. Suga, M. Taniguchi, M. Fujisawa, H. Kanzaki, A. Fujimori, H. Daimon, Y. Ueda, K. Kosuge, and S. Kachi, Phys. Rev. B **41**, 4993 (1990).
[20] E. Goering, M. Schramme, O. Müller, R. Barth, H. Paulin, M. Klemm, M. L. denBoer, and S. Horn, Phys. Rev. B **55**, 4225 (1997).
[21] K. Okazaki, H. Wadati, A. Fujimori, M. Onoda, Y. Muraoka, and Z. Hiroi, Phys. Rev. B **69**, 165104 (2004).
[22] T. C. Koethe, Z. Hu, M. W. Haverkort, C. Schüßler-Langeheine, F. Venturini, N. B. Brookes, O. Tjernberg, W. Reichelt, H. H. Hsieh, H.-J. Lin, C. T. Chen, and L. H. Tjeng, Phys. Rev. Lett. **97**, 116402 (2006).
[23] M. M. Qazilbash, M. Brehm, B.-G. Chae, P.-C. Ho, G. O. Andreev, B.-J. Kim, S. J. Yun, A. V. Balatsky, M. B. Maple, F. Keilmann, H.-T. Kim, and D. N. Basov, Science **318**, 1750 (2007).
[24] M. Taguchi, A. Chainani, N. Kamakura, K. Horiba, Y. Takata, M. Yabashi, K. Tamasaku, Y. Nishino, D. Miwa, T. Ishikawa, S. Shin, E. Ikenaga, T. Yokoya, K. Kobayashi, T. Mochiku, K. Hirata, and K. Motoya, Phys. Rev. B **71**, 155102 (2005).
[25] N. Kamakura, M. Taguchi, A. Chainani, Y. Takata, K. Horiba, K. Yamamoto, K. Tamasaku, Y. Nishino, D. Miwa, E. Ikenaga, M. Awaji, A. Takeuchi, H. Ohashi, Y. Senba, H. Namatame, M. Taniguchi, T. Ishikawa, K. Kobayashi, and S. Shin, Europhys. Lett. **68**, 557 (2004).
[26] K. Horiba, M. Taguchi, A. Chainani, Y. Takata, E. Ikenaga, D. Miwa, Y. Nishino, K. Tamasaku, M. Awaji, A. Takeuchi, M. Yabashi, H. Namatame, M. Taniguchi, H. Kumigashira, M. Oshima, M. Lippmaa, M. Kawasaki, H. Koinuma, K. Kobayashi, T. Ishikawa, and S. Shin, Phys. Rev. Lett. **93**, 236401 (2004).
[27] G. Panaccione, M. Altarelli, A. Fondacaro, A. Georges, S. Huotari, P. Lacovig, A. Lichtenstein, P. Metcalf, G. Monaco, F. Offi, L. Paolasini, A. Poteryaev, O. Tjernberg, and M. Sacchi, Phys. Rev. Lett. **97**, 116401 (2006).
[28] P. S. Cornaglia and A. Georges, Phys. Rev. B **75**, 115112 (2007).
[29] M. van Veenendaal, Phys. Rev. B **74**, 085118 (2006).
[30] M. P. Seah and W. A. Dench, Surf. Interface Anal. **1**, 2 (1979).
[31] Y. Takata, M. Yabashi, K. Tamasaku, Y. Nishino, D. Miwa, T.

Ishikawa, E. Ikenaga, K. Horiba, S. Shin, M. Arita, K. Shimada, H. Namatame, M. Taniguchi, H. Nohira, T. Hattori, S. Sodergen, B. Wannberg, and K. Kobayashi, Nucl. Instrum. Methods Phys. Res. A **547**, 50 (2005).

[32] Y. Muraoka and Z. Hiroi, Appl. Phys. Lett. **80**, 583 (2002).

[33] T. Ishikawa, K. Tamasaku, and M. Yabashi, Nucl. Instrum. Methods Phys. Res. A **547**, 42 (2005).

[34] K. Horiba, N. Kamakura, K. Yamamoto, K. Kobayashi, and S. Shin, J. Electron Spectrosc. Relat. Phenom. **144-147**, 1027 (2005); H. Ohashi, Y. Senba, H. Kishimoto, T. Miura, E. Ishiguro, T. Takeuchi, M. Oura, K. Shirasawa, T. Tanaka, M. Takeuchi, K. Takeshita, S. Goto, S. Takahashi, H. Aoyagi, M. Sano, Y. Furukawa, T. Ohata, T. Matsushita, Y. Ishizawa, S. Taniguchi, Y. Asano, Y. Harada, T. Tokushima, K. Horiba, H. Kitamura, T. Ishikawa, and S. Shin, AIP Conf. Proc. **879**, 523 (2007).

[35] P. Krüger, M. Taguchi, J. C. Parlebas, and A. Kotani, Phys. Rev. B **55**, 16466 (1997).

[36] M. Hamera, W. Walukiewicz, D. D. Nolte, and E. E. Haller, Phys. Rev. B **39**, 10114 (1989); X. M. Chen and A. W. Overhauser, *ibid.* **43**, 14182 (1991).

[37] R. J. O. Mossanek and M. Abbate, Phys. Rev. B **74**, 125112 (2006).

[38] A. Liebsch, H. Ishida, and G. Bihlmayer, Phys. Rev. B **71**, 085109 (2005).

[39] S. J. Oh, J. W. Allen, I. Lindau, and J. C. Mikkelsen, Jr., Phys. Rev. B **26**, 4845 (1982); L. H. Tjeng, C. T. Chen, J. Ghijsen, P. Rudolf, and F. Sette, Phys. Rev. Lett. **67**, 501 (1991).

[40] For a review, see J. W. Allen, in *Techniques*, Synchrotron Radiation Research, Advances in Surface and Interface Science Vol. 1, edited by R. Z. Bachrach (Plenum, New York, 1992), p. 253.

[41] J.-H. Park, Ph.D. thesis, The University of Michigan, 1993; Y. Tezuka, S. Shin, T. Uozumi, and A. Kotani, J. Phys. Soc. Jpn. **66**, 3153 (1997).